

Model-Free Adaptive Optimal Control of Sequential Manufacturing Processes using Reinforcement Learning

Johannes Dornheim · Norbert Link · Peter Gumbsch

Received: date / Accepted: date

Abstract A self-learning optimal control algorithm for sequential manufacturing processes with time-discrete control actions is proposed and evaluated on a simulated deep drawing process. The control model is built during consecutive process executions under optimal control via Reinforcement Learning, using the measured product quality as reward after each process execution. Prior model formulation, which is required by state-of-the-art algorithms like Model Predictive Control and Approximate Dynamic Programming, is therefore obsolete. This avoids several difficulties namely in system identification, accurate modelling, and runtime complexity, that arise when dealing with processes subject to nonlinear dynamics and stochastic influences. Instead of using pre-created process and observation models, value function-based Reinforcement Learning algorithms build functions of expected future reward, which are used to derive optimal process control decisions. The expectation functions are learned online, by interacting with the process. The proposed algorithm takes stochastic variations of the process conditions into account and is able to cope with partial observability. A Q-learning-based method for adaptive optimal control of partially observable fixed-horizon manufacturing

processes is developed and studied. The resulting algorithm is instantiated and evaluated by applying it to a simulated stochastic optimal control problem in metal sheet deep drawing.

Keywords Adaptive Optimal Control · Model-Free Optimal Control · Manufacturing Process Optimization · Reinforcement Learning

1 Introduction

The sequential manufacturing processes considered here are nonlinear stochastic systems which are sequentially executed in order to manufacture products or intermediate goods. Based on the measured quality of the process result, costs are assigned at the end of each execution. The control effort can be reflected by intermediate costs. The goal is to find a controller that minimizes the cost and thereby optimizes the process performance regarding the resulting product quality and the process efficiency. Processes considered here are not fully observable. Current sensor observations are not sufficient for deriving optimal control decisions, therefore historic information has to be taken into account. In addition, no prior information, (like reference trajectories, a process model or an observation model) is given and the optimal control has to be learned during execution.

Model-free adaptive algorithms do not require a priori models and can be used if no accurate process model is available or the use of the given process model for optimization is impractical [24]. In the following, we present different approaches to optimal control and introduce related work.

Johannes Dornheim
Institute Intelligent Systems Research Group, Karlsruhe University of Applied Sciences
Moltkestr. 30, D-76133 Karlsruhe, Germany
Tel.: +49 721 925-2346
E-mail: johannes.dornheim@hs-karlsruhe.de

Norbert Link
Institute Intelligent Systems Research Group, Karlsruhe University of Applied Sciences

Peter Gumbsch
Institute for Applied Materials (IAM-CMS), Karlsruhe Institute of Technology

1.1 Model-Based Optimal Control

For a given process model and cost function, the optimal control problem can be solved offline, using methods from Dynamic Programming [4]. Such approaches are subject to the so-called *curse of dimensionality* in high-dimensional state spaces, leading to difficulties in terms of sample size and computational complexity. In the case of continuous (and thus infinite) state spaces, the optimal control solution by Dynamic Programming requires discretization of the state space, leading to sub-optimal solutions. These problems are addressed in the field of *Approximate Dynamic Programming*, combining Dynamic Programming with function approximation [17].

A family of methods for *online* optimal control that is often applied to industrial processes, is *Model Predictive Control* (MPC). An extensive overview of MPC, and implementation examples of MPC for industrial processes can be found in [6]. Qin et al. [18] provide a survey of industrial grade MPC products. Like Approximate Dynamic Programming, MPC requires a process model, usually determined by linear system identification methods. While MPC with linear models has been explored extensively, nonlinear MPC is an active field of research [13]. The online computational costs in MPC depend on the performance of the prediction model and can be reduced by *offline* pre-calculations as in the *explicit MPC* method [2], or by using *artificial neural networks* to approximate the prediction model [20], [1].

The application of model-based optimal control methods is limited by the quality of the underlying process model. The process identification of highly nonlinear processes from experimental data is very resource and time-consuming. The experiments can alternatively be simulated by using the Finite Element Method (FEM) with a nonlinear material model and can be used for simulation-based process identification. Published examples for the use of FEM models for model-based optimal control include [21] and [5]. In [21], various Approximate Dynamic Programming methods are applied to an optimal control problem of FEM simulated deep drawing processes. In [5], methods from Nonlinear MPC in combination with FEM calculations are used for optimal control of a glass forming process. However, accurate simulation models of nonlinear manufacturing processes are usually quite computationally demanding and are thus rarely used in recent work. Simulation efforts lead to high offline costs when using Approximate Dynamic Programming and extensive online costs when using MPC. From a data-sampling point of view, the use of a general process model (which may represent possible process conditions like tool wear, fluctuating

material properties or stochastic outer conditions and disturbances) is intractable.

1.2 Model-Free Optimal Control

Due to the difficulties inherent in model-based optimal control, we pursue a model-free method for adaptive optimal control of partially observable manufacturing processes. Adaptive online learning of optimal control policies without the need for a-priori knowledge (in the form of process or observation models) is accomplished by *Reinforcement Learning* (RL) [25] and the closely related *Adaptive Dynamic Programming* [27].

Instead of solving the optimal control problem by using an existing process model, model-free optimal control methods optimize the control policy online, while interacting with the process. Due to online learning, model-free methods for optimal control are inherently adaptive, whereas, according to [12], approaches for adaptive MPC focus on robustness and tend to be conservative. The absence of a process model in RL also results in online performance advantages over MPC and in the ability to handle nonlinear systems. The horizon of costs taken into account in RL is usually unbounded, while in MPC it is bounded by the chosen prediction horizon. One advantage of MPC over RL, however, is the ability to handle state constraints and feasibility criteria. MPC (unlike ML) has a mature theory of robustness and stability. These relations between MPC and RL are studied in depth in [12].

The basis of many successful value function-based RL algorithms is the use of general function approximation algorithms (e.g. artificial neural networks), approximating the expected value functions based on experience data, stored in a so-called *replay memory*. Algorithms following this scheme are *Neural Fitted Q-Iteration* [19] and the more recent *Deep Q-Learning* [16]. While in Neural Fitted Q-Iteration artificial neural networks are retrained from scratch regularly, in *Deep Q-Learning* the artificial neural networks are constantly redefined based on mini-batch samples uniformly drawn from the replay memory, enabling the computational efficient use of *deep learning* methods.

Although the relations between RL and optimal control have been studied in depth, there is, to the best of our knowledge, no prior reported application of RL to manufacturing process optimal control.

1.3 Partial Observability

Model Predictive Control, Approximate Dynamic Programming, and Reinforcement Learning determine the

optimal control action based on the current process state. In almost all manufacturing processes, the quantities measured in the current state do not unambiguously describe the state with respect to the optimization problem. Observation models are therefore used in Model Predictive Control and Approximate Dynamic Programming to reconstruct the current state from the observation and control history.

When using model-free optimal control methods on partially observable processes, surrogate state descriptions are derived during control for the current state from the history of measurement values. In more complex cases, *Partially Observable Markov Decision Processes* (POMDPs) can be used to model partially observable environments. The solution of a POMDP involves reconstructing the observation probability function and the derived probability distribution over possible current states, the so-called *belief state*, as a surrogate state for solving the optimal control problem. Finding an exact solution of POMDPs is in general intractable. Therefore, approximations of POMDPs, e.g. *point-based solver* approaches [22] are used. Alternatively, sequence models such as *Recurrent Neural Networks* (RNNs) are used for deriving surrogate states from the observation and control history ([14], [3], [22]).

1.4 Application

We use the optimal control of a deep drawing process as application example and as evaluation case. Besides fixed value parameters, like the initial blank shape and thickness variation, time-variation of blank holder forces are crucial for the resulting process quality. The influence of space and time variation schemes of blank holder forces on the process results is examined e.g. in [26], [23] and [29].

Research on optimal blank holder force control can be found in the publications of Senn et al. ([21]) and Endelt et al. ([10], [9]). In [21], Approximate Dynamic Programming is used for the calculation of an optimal blank holder force controller based on a process model, which is learned on FEM simulation results. A proportional optimal feedback control loop, optimizing blank holder forces regarding a reference blank draw-in, is presented in [10]. In [9], the control loop is embedded in an outer iterative learning algorithm control loop. The iterative learning algorithm transfers information between deep drawing executions for linear adaption of non-stationary process behavior.

unlike the model-free approach proposed, in [21], a process model is used for optimization. In [9], a linear relationship between the error signal and the optimal control and a non-delayed error signal (the distance to a

reference draw-in) is assumed. Both algorithms are optimizing the control based on previously sampled data, while the proposed approach optimizes during control and is thereby able to adapt to unexpected changes of process behavior and conditions.

1.5 Paper Organization

In this paper, we develop the optimal online control of partially observable, nonlinear sequential processes with a delayed cost signal based on Reinforcement Learning, and study it on a deep drawing process. The model-free optimal control approach we propose is based on Neural Fitted Q-Iteration [19], adapted for use in optimal control of stochastic, partially observable and sequential manufacturing processes.

The paper is structured as follows. Chapter 2 introduces the methodical background and algorithms. In chapter 3, the problem of adaptive optimal control of sequential manufacturing processes is described and specified formally. Chapter 4 presents the proposed Reinforcement Learning approach. In chapter 5, the evaluation case, a simulated stochastic and partially observable deep drawing optimization problem, is described and in the final chapter, we discuss quantitative and qualitative results of our approach for the evaluation case.

2 Background

2.1 Markov Decision Processes

The framework of Markov Decision Processes (MDP) is used to model time-discrete decision optimization problems and constitutes the formal basis of algorithms from Dynamic Programming, Adaptive Dynamic Programming, and Reinforcement Learning. An MDP is described by a 5-tuple (X, U, P, R, γ) , where X is the set of states x , U is the set of control actions u , $P_u(x, x')$ is the probability of a transition to x' when applying the control action u in state x , $R_u(x, x')$ is a reward signal given for the transition from state x to x' due to action u , and γ is a discount factor representing the relative weight decrease of future rewards. By definition an MDP satisfies the *Markov property*: The probability of an upcoming state x' depends only on the current state x and on action u and is conditionally independent of previous states and actions.

The goal of decision optimization algorithms is to solve a given MDP by finding an optimal policy $\pi^* : X \rightarrow U$, a function mapping from states to actions with the property that, when following π^* starting in

the state x , the expected discounted future reward $V(x)$ is maximized.

2.2 Optimal Control and the Bellman Equation

Consider the nonlinear time-discrete system

$$x' = f(x, u, w). \quad (1)$$

According to the MDP definition in 2.1, x is a vector of system state variables, u is the control vector. x' denotes the system state following x under u and w , where $w \sim W$ is a random variable of stochastic process conditions, which are independent of previous time steps.

An optimal control problem for the nonlinear system f , for a defined cost-function $C(x, u, x')$, hidden conditions w and for γ -discounted future reward, can be solved by calculating the solution V^* of the Bellman equation (eq. 2), also named *cost-to-go function* in Dynamic Programming.

$$V^*(x) = \min_{u \in U} \mathbb{E}_{w \sim W} [C(x, u, x') + \gamma V^*(x')] \quad (2)$$

The term C is a local cost function depending on the state x' and, in some applications, also on the previous state x and the control vector u that leads to the state. When eq. (2) is solved, the optimal control law $\pi^*(x)$ can be extracted by $\arg \min_{u \in U} \mathbb{E}_{w \sim W} [V^*(x')]$ for a given process model f .

In this paper, following the standard notation of Reinforcement Learning, the system f and the optimization problem are modeled as an MDP as introduced in the previous chapter. In MDPs, instead of the cost-function C , a reward function R is used, leading to a maximization problem instead of the minimization in eq. (2). The Bellman equation is then given by

$$V^*(x) = \max_{u \in U} \mathbb{E}_{x'} [R_u(x, x') + \gamma V^*(x')], \quad (3)$$

where the probability of x' is given by the transition probability function $P_u(x, x')$, capturing stochastic process conditions w .

2.3 Q-Learning

The objective of Q-learning [28] is to find the optimal Q-function

$$Q^*(x, u) = \mathbb{E}_{x'} [R_u(x, x') + \gamma \max_{u' \in U} Q^*(x', u')]. \quad (4)$$

Unlike the *optimal value function* in (3), the Q-function is defined over state, action tuples (x, u) . By taking actions into account, the Q-function implicitly captures the system dynamics, and no additional system model is needed for optimal control. Once the optimal Q-function has been found, the optimal control policy π^* is given by

$$\pi^*(x) = \arg \max_{u \in U} Q^*(x, u). \quad (5)$$

In Q-learning-based algorithms, Q^* is found by constantly updating a Q^* -approximation Q' by the update step in eq. 6, using *experience tuples* (x, u, x', R) and a given learning rate $\alpha \in [0, 1]$, while interacting with the process in an explorative manner.

$$Q'(x, u) = (1 - \alpha)Q(x, u) + \alpha(R + \gamma \max_{u' \in U} Q(x', u')) \quad (6)$$

3 Problem Description

In this paper, we consider sequential manufacturing processes. The processing of a single workpiece involves a constant number of discrete control steps and can be modeled as a fixed-horizon *Markov Decision Process* (MDP), where for every policy and every given start state, a terminal state is reached at time step T . Each processing may be subject to slightly different conditions (e.g. the initial workpiece, lubrication, tool wear). In Reinforcement Learning, the control of a finite-horizon MDP from the start to the terminal state (here: single workpiece processing) is denoted as *episode*, and tasks with repeated execution of episodes are denoted as *episodic tasks*. Hereafter, the term *episode* is used in Reinforcement Learning contexts, and the phrase *process execution* in manufacturing contexts.

Most processes, such as forming or additive manufacturing, are irreversible. The related control decisions are leading to disjoint sub-state-spaces X_t depending on the time step $t < T$. The terminal state reached (x_T) is assessed, and the main reward is determined by the final product quality, quantified by a cost function. At each time step during process execution, a negative reward can also be assigned according to cost arising from the execution of a dedicated action in the present state. For deterministic processes, where the process dynamics are solely dependent on the control parameters u , the structure of the fixed-horizon processing MDP is represented by a tree graph with the starting state as root vertex and the terminal states as leaf vertices. In the manufacturing process optimal control case considered in this paper, the process dynamics during an

individual process execution are dependent on stochastic per-episode process conditions. In this scenario, the underlying MDP equals a collection of trees, each representing a particular process condition setting. An exemplary MDP tree is depicted on the right-hand side of fig. 2, relating to the optimal control of the blank holder force in deep drawing.

3.1 Deep Drawing, Blank Holder Force Optimization

A controlled deep drawing process is used as a proof of concept, where the optimal variation of the blank-holder force is determined at processing time. As emphasized in 1.4, the result of the deep drawing process is strongly dependent on choosing appropriate blank holder force trajectories. In this paper, the optimization problem is modeled according to the described sequential Manufacturing Process MDP framework. Parameterizable FEM models are used to simulate the online process behavior for method development and evaluation. The simulated problem setting (*environment*) is depicted in fig. 1. The current environment state x is calculated by the FEM model based on the given control action u , the previous environment-state and process conditions s , which are randomly sampled from a given distribution. Based on x , the current reward R is derived by a reward function, and observable values o are derived by a sensor model. The (R, o) tuple is finally reported to the control agent. A detailed description of the simulation model and the environment parameters used in this work is provided in chapter 5.1.

4 Approach

A generic version of the Q-learning control agent is depicted in fig. 1. An observer derives surrogate state descriptions \bar{x} from the observable values o , and previous control actions u . Control actions are determined based on a policy π , which itself is derived from a Q-function. In the approach proposed, the Q-function is learned from the processing samples via batch-wise retraining of the respective function approximation, following the incremental variant of the neural fitted Q iteration approach ([19]).

For exploration, an ϵ -greedy policy is used, acting randomly in an ϵ -fraction of control actions. To derive the optimal action, the current approximation of the Q^* -function is used (exploitation). The exploration factor $\epsilon \in [0, 1]$ is decreased over time to improve the optimization convergence and to reduce the number of sub-optimal control trials. We use an exponential decay

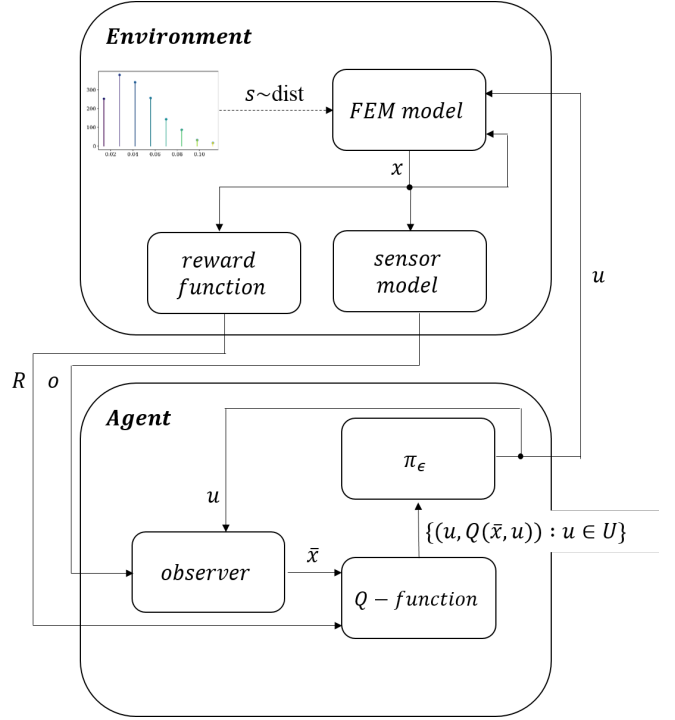


Fig. 1 Scheme of the interaction of the proposed optimal online control agent with the simulated process environment.

over the episodes i according to $\epsilon_i = \epsilon_0 e^{-\lambda i}$, with decay rate λ .

4.1 Handling Partial Observability

As described in 1.3, due to the partial observability of process states, the current optimal action is potentially dependent on the whole history of observables and actions. In the case of fixed horizon problems, like episodes of the sequential manufacturing processes considered here (see 3), the current history is limited to the current episode only.

The optimal control of a partially observable process depends on the given information. If representative data of observables and corresponding state values can be drawn from the underlying observation probability function O (as assumed in [21]) an explicit observation model can be learned and used to derive state values and apply regular MDP solution methods. If no prior information about the state space and observation probabilities is available, surrogate state descriptions \bar{x} have to be derived from the history of observable values and control actions.

A necessary condition for finding the optimal control policy π^* for the underlying MDP based on \bar{X} is, that the π^* is equivalent for any two states (x_1, x_2) , whose corresponding action observable histories

are mapped to the same surrogate state \bar{x} . The fulfillment of this condition is restricted by observation (measurement) noise. In the present stochastic fixed horizon case, the information about the state contained in the observable and action history is initially small but increases with every control and observation step along the episode. The condition is therefore violated, especially in the beginning of an episode.

In this work, we use the full information about observables and actions for the current episode by concatenating all these values into $\bar{\mathbf{x}}$. Thus, the dimension of $\bar{\mathbf{x}} \in \mathbb{R}^n$ is time-dependent according to $n_t = [\dim(O) + \dim(U)] * t$. When using Q-function approximation, the approximation model input dimension is therefore also dependent on t . If function approximation methods with fixed input dimensions (like standard artificial neural networks) is used, a dedicated model for each control step is required. This complicates the learning process in cases with higher numbers of control-steps, especially for retraining and hyperparameter optimization. These problems can be avoided by projection to a fixed dimension surrogate state vector $\bar{\mathbf{x}}$, e.g. via Recurrent Neural Networks.

4.2 Q Function Approximation

The incorporation of function approximation into Q-learning allows for a generalization of the Q-function over the (X, U) -space. Thus it becomes possible to transfer information about local Q-values to newly observed states x . Approximating the Q-function is, therefore, increasing the learning speed in general and, furthermore, enables an approximate representation of the Q-function in cases with a continuous state space.

In this paper, artificial neural networks are used for regression, which are retrained every k episodes, based on data from a so-called replay memory. The replay memory consists of an increasing set of experience tuples $(\bar{x}, u, \bar{x}', R)$, gathered during processing under control with the explorative policy described at the beginning of chapter 4. The Q-function is re-trained from scratch by using the complete replay-memory periodically. This is in contrast to standard Q-learning, where the Q-function is re-defined after each control action u based on the current experience tuple $(\bar{x}, u, \bar{x}', R)$ only. Due to the non-stationary sampling process in Reinforcement Learning, the use of standard Q-learning in combination with iteratively trained function approximation can result in a complete loss of experience (*catastrophic forgetting*) [11]. Using a replay memory for periodic retraining of Q-function approximation models has shown to be more stable and data-efficient [19].

As described in 4.1, the dimension of the used state representation \bar{x} is dependent on the current control step $t \in [0, 1, \dots, T]$. Because the input dimension of feed-forward artificial neural networks is fixed, multiple artificial neural networks $Q_t(\bar{x}, u, \Theta_t)$, with weight parameter values Θ_t , depending on the current control step t are used. For each tuple $(\bar{x}, u, \bar{x}', R)$ in the replay-memory, the Q-values are updated before retraining according to eq. (6). The update is based on the Q-approximation for the current step, $Q_t(\bar{x}, u, \Theta_t)$, and the Q-function approximation for $t+1$, $Q_{t+1}(\bar{x}', u', \bar{\Theta}_{t+1})$, where Θ_t are weight values for time step t from the previous training iteration and $\bar{\Theta}_t$ are weight values, already updated in the current training iteration. The per-example loss used for training is the squared error

$$L((x, u), y, \Theta_t) = (y - Q_t(x, u, \Theta_t))^2, \quad (7)$$

where the training target y for a given replay memory entry is defined by

$$y = (1-\alpha)Q_t(\bar{x}, u, \Theta_t) + \alpha \left[R + \gamma \max_{u' \in U} Q_{t+1}(\bar{x}', u', \bar{\Theta}_{t+1}) \right]. \quad (8)$$

The proposed update mechanism works backward in the control steps t and thereby, as shown in eq. (8), incorporates the already updated parameters for Q_{t+1} when updating Q_t . Thereby, the propagation of reward information is accelerated, leading to a faster convergence as shown in the results section (chapter 6).

At the beginning of a process, the observable values only depend on the externally determined initial state, which in our case does not reflect any process influence. The Q-function Q_0 then has to be defined over the single state ϕ and therefore only depends on the control action u_0 . In contrast to other history states, one transition sample (ϕ, u_0, \bar{x}_1) involving ϕ is stored in the replay memory per episode. By assuming that the stored transition-samples are representative of the transition probability function $p(\bar{x}_1 | \phi, u_0)$, the expected future reward for the first control-step u_0 (here denoted as Q_0) is defined in eq. (9) and can be calculated directly by using the replay memory and the approximation model for Q_1 .

$$Q_0(\phi, u_0) = \mathbb{E}_{\bar{x}_1} \left[R + \gamma \max_{u_1} Q_1(\bar{x}_1, u_1) \right] \quad (9)$$

5 Evaluation Environment

The approach presented in the previous chapters is evaluated by applying it to optimize the blank holder forces

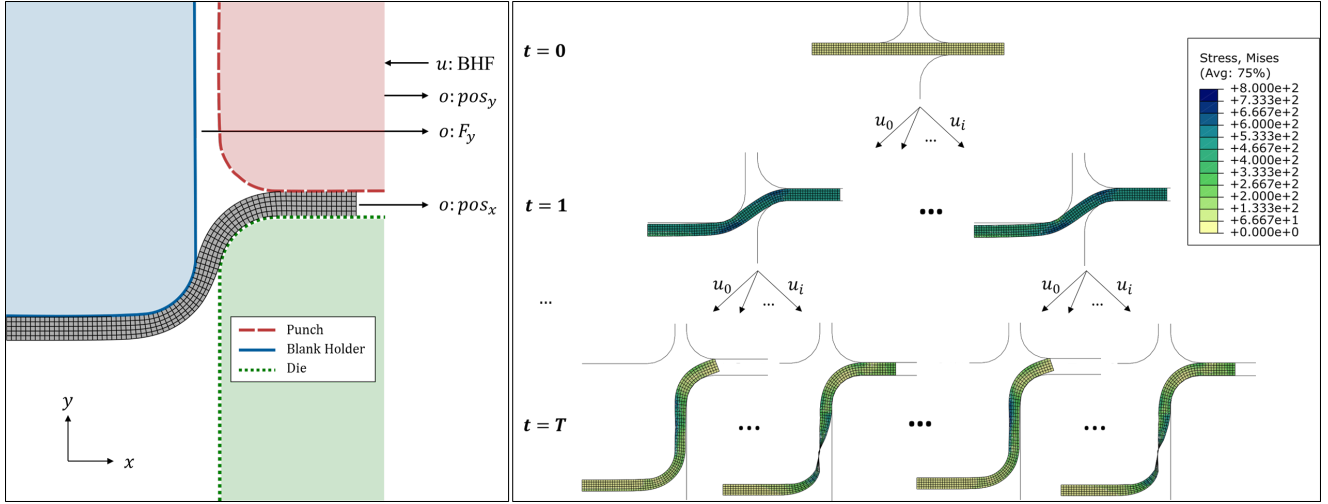


Fig. 2 left: Rotationally symmetric deep drawing simulation model with observable values o and actor values u . right: tree-like manufacturing process MDP for a given friction coefficient of 0.056, with color coded von Mises stress distribution (unit: MPa) in the radial workpiece intersection.

during deep drawing processes. A controlled evaluation environment is implemented by using numerical simulations of the process. The digital twin of a deep drawing process is realized via FEM simulation and used for the online process control assessment. The simulation model, as depicted on the left-hand side of fig. 2, simplifies the deep drawing process assuming rotational symmetry and isotropic material behavior. Due to its simplicity, the FEM model is very efficient with respect to computing time (about 60 seconds simulation-time per time step on 2 CPU cores) it, therefore, enables in-depth methodological investigations such as comparative evaluations of different algorithms and parameter settings.

Abaqus FEM code was used for this work. Extensive use of the Abaqus scripting interface [8] in combination with analysis restarts (compare [7], chapter 9.1.1) has been made for the efficient and reusable simulation of an online optimal control setting, where the control agent sets control parameters based on current state observables.

5.1 FEM Model

The rotationally symmetric FEM model, visualized on the left-hand side of fig. 2, consists of three rigid parts interacting with the deformable blank. The circular blank has a thickness of 25 mm and a diameter of 400 mm. An elastic-plastic material model is used for the blank, which models the properties of Fe-28Mn-9Al-0.8C steel [30]. The punch pushes the blank with constant speed into the die, to form a cup with a depth of 250 mm. Blank holder force values can be set at the beginning of

each of five consecutive control steps, where the blank holder force changes linearly in each control step from its current value to the value given at the start of the step. Blank holder force can be chosen from the set $\{20 \text{ kN}, 40 \text{ kN}, \dots, 140 \text{ kN}\}$ in each control step. The initial blank holder force is 0.0 kN.

5.2 Process Disturbances

Stochastic process disturbances and observation noise are added to the simulated deep drawing process described in 5.1 to create a more realistic process twin. Process disturbances are introduced by stochastic contact friction. The friction coefficient is modeled as a beta-distributed random variable, sampled independently for each deep drawing process execution (episode). The distribution parameters are chosen to be $\alpha = 1.75, \beta = 5$. The distribution is rescaled to the range $[0, 0.14]$. For better reusability of simulation results, the friction coefficient is discretized into 10 bins of equal size. The resulting distribution is discrete and defined over 10 equidistant values from the interval $[0.014, 0.14]$. The distributions mode is 0.028.

5.3 Partial Observability

As depicted in fig. 1, the current process state x is dependent on the previous state, the control action u and the current friction coefficient s . Neither the state x nor the underlying beta-distribution is accessible by the agent. Instead, three observable values o are provided in each time step:

- the current stamp force
- the current blank infeed in the x-direction
- the current offset of the blank-holder in the y-direction

The measurement noise of these observables is assumed to be additive and to follow a normal distribution, where the standard deviation is chosen to 1% of the respective value range for both the stamp force and the blank holder offset and 0.5% of the value range for the blank infeed. This corresponds to common measurement noise characteristics encountered in analogue sensors.

5.4 Reward Function

As described in 2.2, the reward function can be composed of local cost (related to the state and action of each single processing step) and of global cost (assigned to the process result or final state). In the case of zero or constant local cost, the optimization is determined by the reward assigned to the terminal state, which is assessed by a quality control station. For our evaluation, we consider this case. The process goal is to produce a cup with low internal stress and low material usage, but with sufficient material thickness.

FEM elements e of the blank are disposed in the form of a discretization grid with n columns and m rows, depicted in fig. 2. For the reward calculation, three $n \times m$ matrices (\mathbf{S} , \mathbf{W}^y , \mathbf{D}^x) of element-wise simulation results are used. Where \mathbf{S}_{ij} is the mean *von Mises Stress* of element e_{ij} , \mathbf{W}_{ij}^y is the width of element e_{ij} in y-direction and \mathbf{D}_{ij}^x is the x -axis displacement of element e_{ij} between time step 0 and T . Using these matrices, the reward is composed of the following three terms based on the simulation results: (a) The l^2 -norm of the vectorized von Mises stress matrix $C_a(x_T) = \|\text{vec}(\mathbf{S})\|$, (b) the minimum $C_b(x_T) = -\min(\mathbf{s}_i)$ over a vector \mathbf{s} of column-wise summed blank widths $\mathbf{s}_i = \sum_j w_{ij}^y$ and (c) The summed displacement of elements in the last column $C_c(x_T) = \sum_j d_{nj}^x - d_{nj}^x$, representing material consumption during drawing. The reward function terms R_i are scaled according to eq. 10, with $C_i, i \in \{a, b, c\}$, resulting in approximately equally balanced R_i .

$$R_i(x_T) = 10 * \left(1 - \frac{C_i(x_T) - C_i^{\min}}{C_i^{\max} - C_i^{\min}} \right) \quad (10)$$

The extrema C_i^{\min} and C_i^{\max} are empirically determined per cost term, using 100 data tuples from terminal states, sampled in prior experiments by applying random blank holder force trajectories. The final reward is the weighted harmonic mean if all resulting

terms R_i are positive, and 0 otherwise.

$$R(x_T) = \begin{cases} H(x_T, W), & \text{if } \forall i \in \{a, b, c\} : R_i(x_T) \geq 0 \\ 0, & \text{otherwise} \end{cases} \quad (11)$$

$$H(x_T, W) = \frac{\sum_i w_i}{\sum_i \frac{w_i}{R_i(x_T)}} \quad (12)$$

The harmonic mean was chosen to give preference to process results with balanced properties regarding the reward terms. The weights of the harmonic mean can be used to control the influence of cost terms to the overall reward. Equal weighting is used for the evaluation experiments of the presented algorithms.

5.5 Q-Function Representation

The Q-function, as introduced in chapter 4.2, is represented by a set of feedforward artificial neural networks, which are adapted via the backpropagation algorithm. The optimization uses the sum-of-squared-error loss function combined with an l^2 weight regularization term. The limited-memory approximation to the *Broyden-Fletcher-Goldfarb-Shanno* (L-BFGS) algorithm [15] is used for optimization because it has been shown to be very stable, fast converging and a good choice for learning neural networks when only a small amount of data is available. Rectified linear unit functions (ReLU) are used as activation functions in the hidden layers. Two hidden layers are used for all networks, consisting of 10 units each for Q_1 and 50 neurons for Q_2, Q_3, Q_4 , respectively.

6 Results

The approach presented in chapter 4 was investigated with a set of experiments, executed with the simulated deep drawing process described in chapter 5.1. The proposed adaptive optimal control algorithm is compared to non-adaptive methods from standard Model Predictive Control and from Approximate Dynamic Programming. To make them comparable, the non-adaptive methods are based on a given perfect process model which does not capture stochastic process influences. This is reflected by a static friction coefficient of 0.028 in the respective simulation model. The non-adaptive methods are represented by the optimal control trajectory which was determined by a full search over the trajectory-space for the respective simulation. The *expected baseline reward*, which is used for the evaluation plots, is

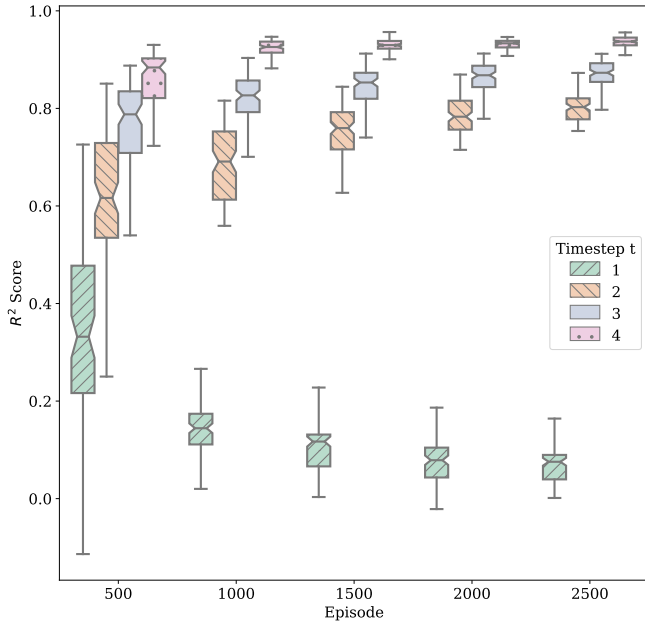


Fig. 3 Cross-Validation R^2 score for Q_t models by episode (quality of the Q-function representation), sorted by t (color)

the expectation value of the reward reached by the determined trajectory in the stochastic setting.

The model retraining interval k was chosen to be 50 process executions (episodes). The first Q -function training is carried out after 50 random episodes. For hyperparameter optimization and evaluation, the performance of the Q -function approximators is evaluated by 5-fold cross-validation during each retraining phase. In fig. 3 the *coefficient of determination* (R^2 -Score), resulting from cross-validation, is plotted over the number of episodes for the neural network hyperparameters described in chapter 5.5 and the following Reinforcement Learning parameters: learning-rate $\alpha = 0.7$, exploration-rate $\epsilon = 0.3$ and ϵ decay $\lambda = 10^{-3}$.

In this case, for $t \in \{2, 3, 4\}$, the R^2 -Score is increasing over time as expected. For the first time step (t_1) however, a decrease of the R^2 -Score over time is observed. No hyperparameters leading to a different convergence behavior for t_1 were found during optimization. Results from experiments, visualized in fig. 7, where the current friction-coefficient can be accessed by the agent, indicate that the decrease is related to the partial observability setting (see chapter 4.1). A deeper analysis of the data shows that, due to the early process stage and measurement noise, the information about the friction-coefficient in the observable values is very low for t_1 . This causes the Q_1 -function to rely mainly on the previous action u_0 and the planned action u_1 . In the first episodes, high exploration rates and low quality Q -functions are leading to very stochastic

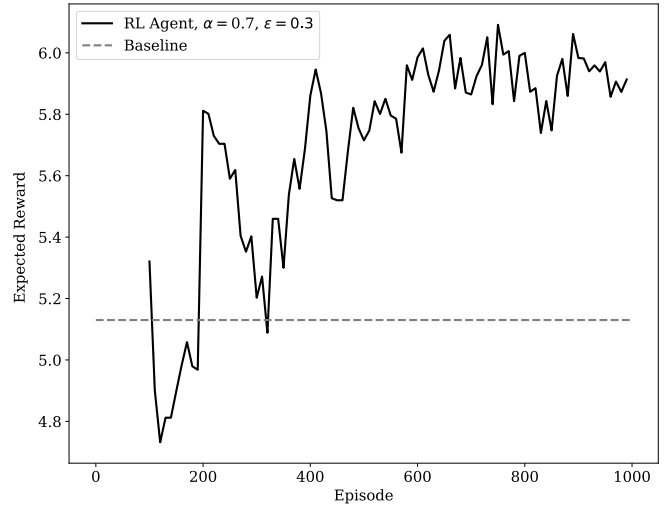


Fig. 4 Expected reward for the RL approach during optimization (black, solid) and expected reward for the baseline approach (grey, dashed)

control decisions and consequently to almost equally distributed values of u_0 and u_1 in the replay memory. In later episodes, optimal control decisions u_0^* and u_1^* ($u_t^* = \arg \max_{u_t \in U} Q^*(x, u_t)$) are increasingly dominant in the replay memory. Due to the low information in the observable values, u_0^* and u_1^* are independent of the friction coefficient. The advantage of the Q_1 model over the simple average on the replay memory is decreasing due to this dominance. Hence, the R^2 -score is shrinking. In the fully observable case (fig. 7), u_0^* and u_1^* are dependent on the friction coefficient, causing the R^2 score of the Q_1 model to increase over time.

Fig. 4 shows results of the Reinforcement Learning control for an exemplary simulated production batch of 1000 deep drawing episodes. The *expected reward* for a given episode and friction denotes the reward reached in the last episode of the previous optimal control, where under the given friction the agent acted optimally (without exploration) according to the current Q -function. The overall expected reward per episode (solid black line) is the expectation value of the friction-dependent expected rewards for the given friction-distribution. The baseline (dashed black line) is the expected reward for non-adaptive methods, determined as described above.

In order to reveal the effect of the learning parameter variation, experiments were conducted with varying learning rates α and exploration rates ϵ to explore their influence on the quality of the online control, reflected by the distribution of the resulting reward. For each parameter combination, 10 independent experimental batches were executed under control of the respectively parameterized Reinforcement Learning algo-

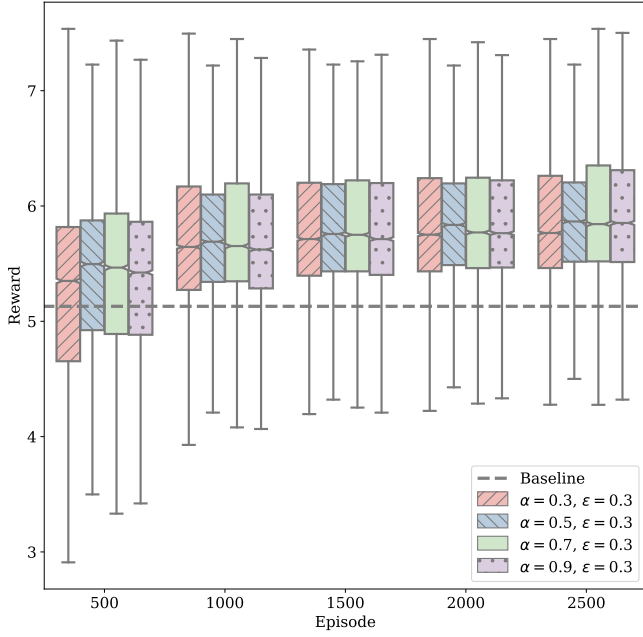


Fig. 5 Reward-distribution by episode for different learning rates α

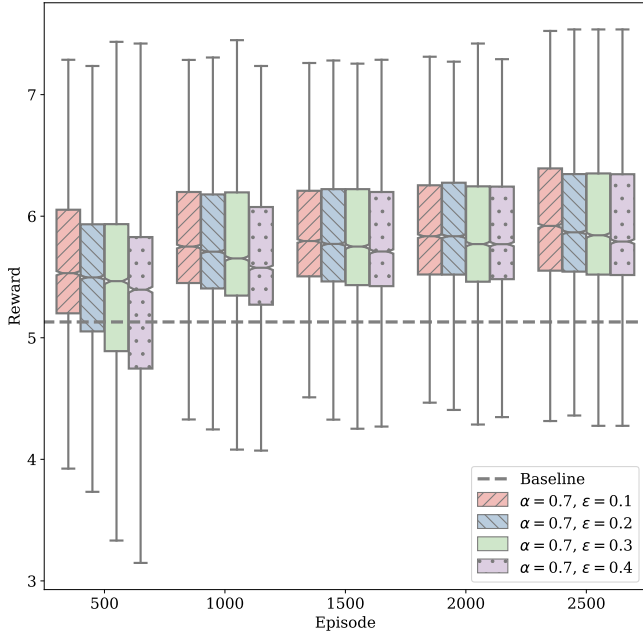


Fig. 6 Reward-distribution by episode for different exploration rates ϵ

algorithm, each with 2500 deep drawing episodes. The resulting reward distribution, sampled into bins of 500 subsequent episodes, is visualized by box plots in fig. 5 for a varying learning rate α and in fig. 6 for various exploration-rates ϵ respectively. In all experiments, an ϵ -decay λ of 10^{-3} and the function approximation hyperparameters described above were used. It can be seen from fig. 5 that the algorithm is not sensitive to

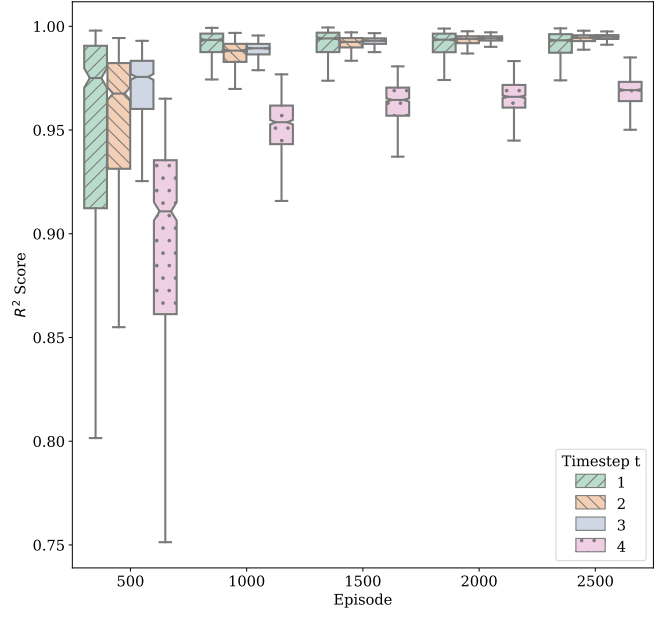


Fig. 7 Cross-Validation R^2 score for fully observable environment (observable friction coefficient)

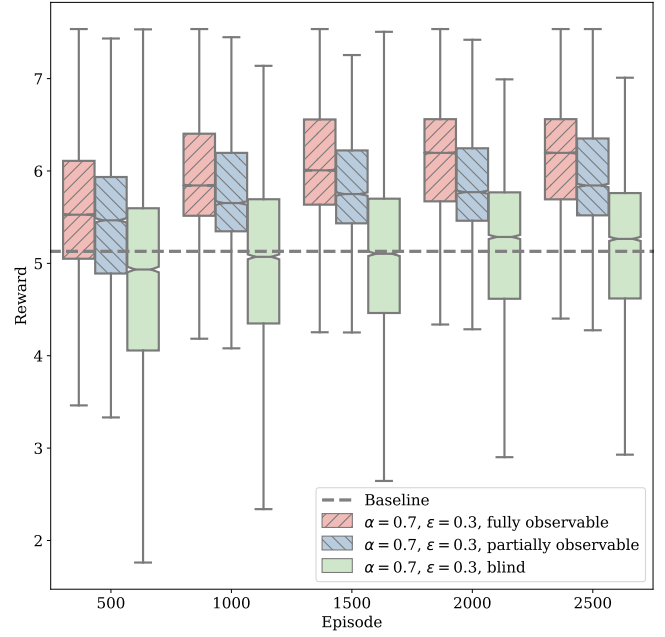


Fig. 8 Reward-distribution by episode for observable friction (red), partially observable (standard case, blue), control based on the Reward-signal only, without using observable values (green)

the chosen parameters but that small and large learning rates yield somewhat less optimal results. The optimization quality, however, decreases slightly with increasing exploration rate as shown in fig. 6. This is due to the negative effect of explorative behavior on the short term outcome of the process. In the deep drawing process considered, even low exploration rates (here:

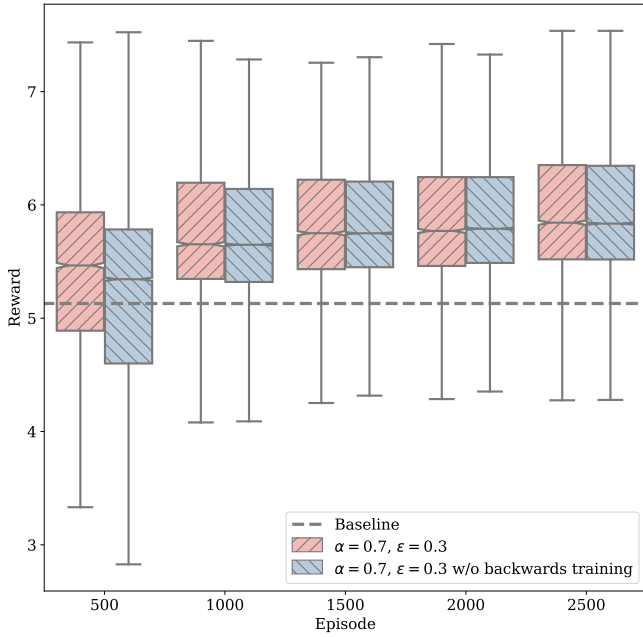


Fig. 9 Reward-distribution by episode for training of Q-networks backwards in time, as described in 4.2 (red) and no backwards training (blue)

0.1) lead to fast overall convergence which is not necessarily the case in more complex applications.

Besides learning parameter variation, experiments were made to investigate the effect of process observability. In fig. 8, the rewards achieved by Reinforcement Learning-based control of 10 independent executions in three different observability scenarios are visualized. In the fully observable scenario (left), the agent has access to the current friction coefficient and thus perfect information about the process state. The partially observable scenario (middle) is equivalent to the scenario described in chapter 4.1 and is used in the previously described experiments. The "blind" agent (right) has no access to the process state, and the optimal control is based on the knowledge about previous control actions and rewards only. In this scenario, the mean control performance after 1000 episodes is comparable to the baseline.

In fig. 9, the effect of training the approximation models backward in control steps (as described in chapter 4.2) is depicted. Training backward in control-steps (left) leads to a faster convergence than retraining without backward training (right).

7 Discussion and Future Work

It has been shown how Reinforcement Learning-based methods can be applied for adaptive optimal control of

sequential manufacturing processes with varying process conditions. A model-free Q-learning-based algorithm has been proposed, which enables the adaptivity to varying process conditions through learning to modify the Q-function accordingly. A class of sequential manufacturing processes has been described, to which this generic method can be applied. The approach has been instantiated for and evaluated with, the task of blank holder force optimal control in a deep drawing process. The optimal control goal was the optimization of the internal stresses, of the wall thickness and of the material efficiency for the resulting workpiece. The deep drawing processes used to evaluate the approach were simulated via FEM. The experimental processes were executed in an automatic virtual laboratory environment, which was used to vary the process conditions stochastically and to induce measurement noise. The virtual laboratory is currently specialized to the deep drawing context but will be generalized and published in future work for experimentation and evaluation of optimal control agents on all types of FEM simulated manufacturing processes.

Contrary to model-based approaches, no prior model is needed when using RL for model-free optimal control. It is therefore applicable in cases where accurate process models are not feasible or not fast enough for online prediction. When applied online, the approach is able to self-optimize, according to the cost function. The approach is able to adapt to instance-specific process conditions and non-stationary outer conditions. In a fully blind scenario, with no additional sensory information, the proposed algorithm reaches the results of non-adaptive model-based methods from Model Predictive Control and Approximate Dynamic Programming in the example use case. The disadvantage of model-free learning approaches, including the proposed Reinforcement Learning (RL) approach, is the dependence on data gathered during the optimization (exploration). Exploration leads to suboptimal behavior of the control agent in order to learn about the process and to improve future behavior. When used for optimal control of manufacturing processes, RL can lead to increased product rejection rates, which decrease during the learning process. Optimal manufacturing process control with RL can be used in applications with high production figures but is not viable for small individual production batches.

To overcome these problems, the incorporation of safe exploration methods from the field of *safe reinforcement learning* could directly lead to decreased rejection rates. Extending the proposed approach with methods from *transfer learning* or *multiobjective reinforcement learning* could enable information transfer

between various process instances, differing e.g. in the process conditions or the production goal, and could thereby lead to more efficient learning, and consequently to decreased rejection rates, and a wider field of application.

Acknowledgements The authors would like to thank the DFG and the German Federal Ministry of Education and Research (BMBF) for funding the presented work carried out within the Research Training Group 1483 Process chains in manufacturing (DFG) and under grant #03FH061PX5 (BMBF).

References

- Åkesson, B.M., Toivonen, H.T.: A neural network model predictive controller. *Journal of Process Control* **16**(9), 937–946 (2006). DOI 10.1016/j.jprocont.2006.06.001
- Alessio, A., Bemporad, A.: A survey on explicit model predictive control. In: *Nonlinear Model Predictive Control: Towards New Challenging Applications*, pp. 345–369. Springer (2009)
- Bakker, B.: Reinforcement Learning with Long Short-Term Memory. In: *Advances in Neural Information Processing Systems*, vol. 14, pp. 1475–1482 (2002)
- Bellman, R.: *Dynamic programming*. Courier Corporation (2013)
- Bernard, T., Moghaddam, E.E.: Nonlinear Model Predictive Control of a Glass forming Process based on a Finite Element Model. *Proceedings of the 2006 IEEE International Conference on Control Applications* pp. 960–965 (2006)
- Camacho, E.F., Alba, C.B.: *Model predictive control*. Springer Science & Business Media (2013)
- Dassault Systèmes: *Abaqus 6.14 Analysis User's Guide: Analysis*, vol. II. Dassault Systèmes (2014)
- Dassault Systèmes: *Abaqus 6.14 Scripting User's Guide*. Dassault Systèmes (2014)
- Endelt, B.: Design strategy for optimal iterative learning control applied on a deep drawing process. *The International Journal of Advanced Manufacturing Technology* **88**(1–4), 3–18 (2017)
- Endelt, B., Tommerup, S., Danckert, J.: A novel feedback control system—controlling the material flow in deep drawing using distributed blank-holder force. *Journal of Materials Processing Technology* **213**(1), 36–50 (2013)
- French, R.M.: Catastrophic forgetting in connectionist networks. *Trends in cognitive sciences* **3**(4), 128–135 (1999)
- Görges, D.: Relations between Model Predictive Control and Reinforcement Learning. *IFAC-PapersOnLine* **50**(1), 4920–4928 (2017). DOI 10.1016/j.ifacol.2017.08.747
- Grüne, L., Pannek, J.: Nonlinear model predictive control. In: *Nonlinear Model Predictive Control*, pp. 43–66. Springer (2011)
- Lin, L.J., Mitchell, T.M.: Reinforcement learning with hidden states. *From animals to animats* **2**, 271–280 (1993)
- Liu, D.C., Nocedal, J.: On the limited memory bfgs method for large scale optimization. *Mathematical programming* **45**(1–3), 503–528 (1989)
- Mnih, V., Kavukcuoglu, K., Silver, D., Rusu, A.A., Veness, J., Bellemare, M.G., Graves, A., Riedmiller, M., Fidjeland, A.K., Ostrovski, G., et al.: Human-level control through deep reinforcement learning. *Nature* **518**(7540), 529 (2015)
- Powell, W.B.: *Approximate Dynamic Programming: Solving the curses of dimensionality*. John Wiley & Sons (2007)
- Qin, S., Badgwell, T.A.: A survey of industrial model predictive control technology. *Control Engineering Practice* **11**(7), 733–764 (2003). DOI 10.1016/S0967-0661(02)00186-7
- Riedmiller, M.: Neural Fitted Q Iteration - First Experiences with a Data Efficient Neural Reinforcement Learning Method. In: *European Conference on Machine Learning*, pp. 317–328. Springer (2005)
- Saint-Donat, J., Bhat, N., McAvoy, T.J.: Neural net based model predictive control. *International Journal of Control* **54**(6), 1453–1468 (1991). DOI 10.1080/00207179108934221
- Senn, M., Link, N., Pollak, J., Lee, J.H.: Reducing the computational effort of optimal process controllers for continuous state spaces by using incremental learning and post-decision state formulations. *Journal of Process Control* **24**(3), 133–143 (2014). DOI 10.1016/j.jprocont.2014.01.002
- Shani, G., Pineau, J., Kaplow, R.: A survey of point-based POMDP solvers. *Autonomous Agents and Multi-Agent Systems* **27**(1), 1–51 (2013). DOI 10.1007/s10458-012-9200-2
- Singh, C.P., Agnihotri, G.: Study of Deep Drawing Process Parameters: A Review. *International Journal of Scientific and Research Publications* **5**(1), 2250–3153 (2015). DOI 10.1016/j.matpr.2017.01.091
- Sutton, R., Barto, A., Williams, R.: Reinforcement learning is direct adaptive optimal control. *IEEE Control Systems* **12**(2), 19–22 (1992). DOI 10.1109/37.126844
- Sutton, R.S., Barto, A.G.: *Reinforcement learning: An introduction*, vol. 1. MIT press Cambridge (1998)
- Tommerup, S., Endelt, B.: Experimental verification of a deep drawing tool system for adaptive blank holder pressure distribution. *Journal of Materials Processing Technology* **212**(11), 2529–2540 (2012). DOI 10.1016/j.jmatprotec.2012.06.015
- Wang, F.y., Zhang, H., Liu, D.: Adaptive Dynamic Programming: An Introduction. *IEEE computational intelligence magazine* **4**(2), 39–47 (2009)
- Watkins, C.J.C.H.: *Learning from delayed rewards*. Ph.D. thesis, King's College, Cambridge (1989)
- Wifi, a., Mosallam, a.: Some aspects of blank-holder force schemes in deep drawing process. *Journal of Achievements in Materials and Manufacturing Engineering* **24**(1), 315–323 (2007)
- Yoo, J.D., Hwang, S.W., Park, K.T.: Factors influencing the tensile behavior of a fe-28mn-9al-0.8 c steel. *Materials Science and Engineering: A* **508**(1–2), 234–240 (2009)